Spectra and Time Evolution of Unstable Hadronic States by the Mittag-Leffler Expansion

UQS 2024, Tohoku University, September 4, 2024

Wren Yamada

RIKEN iTHEMS

PRC 102 055201 (2020), PRD 105 014034 (2022), PRL 129 192001 (2022), PRD 108 L071502(2023)

Contents

Mittag-Leffler Expansion and Near-Threshold Spectrum

- Uniformization: Sphere (2-channel), Torus representation (3-channel)
- Mittag-Leffler Expansion of the 2-channel, 3-channel $\mathcal{S}$-matrix
- $Z_c(3900)$

- Enhanced peak structure indicates the existance of a pole (poles) ”Resonance”: pole on $[bt]_-$, $[bb]_-$, ”Threshold Cusp”: pole on $[tb]_+$

Time Evolution of Unstable states

- Survival Amplitude of Single-channel system
- Extension to the 2-channel system; decay of resonance pole components, ”threshold cusp” pole components

- Non-exponential decay of ”threshold cusp” ($[tb]_+$ pole components)

Mittag-Leffler Expansion to temporal Correlation functions in Euclidean time

- Demonstration with a simple model (ρ meson coupled to $\pi\pi$)

Motive

考えられる多くの peak が、two-body hadron

ている。

- Many candidates of exotic hadrons ($qq\bar{q}\bar{q}$, $qqqq\bar{q}$, . . .) observed in the vicinity of the inelastic 2-body thresholds
  - R. Aaij et al. (LHCb Collaboration), *"Observation of J/ψp Resonances Consistent with Pentaquark States in $\Lambda_b^0 \to J/\psi K^- p$ Decays"*, Phys. Rev. Lett. 115, 072001 (2015)
  - R. Aaij et al. (LHCb Collaboration), *"Observation of a $J/\psi\Lambda$ resonance consistent with a strange pentaquark candidate in $B^- \to J/\psi\Lambda\bar{p}^-$ decays"*, arXiv:2210.10346.

exotic hadron の候補と

threshold に見つかって

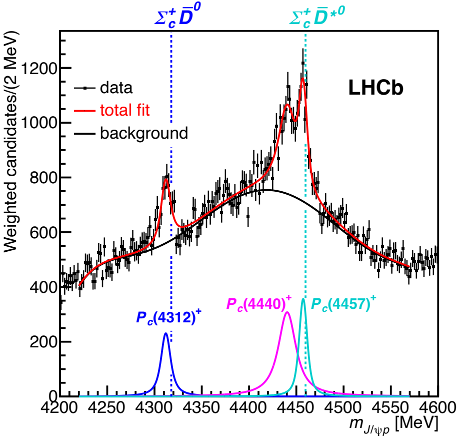

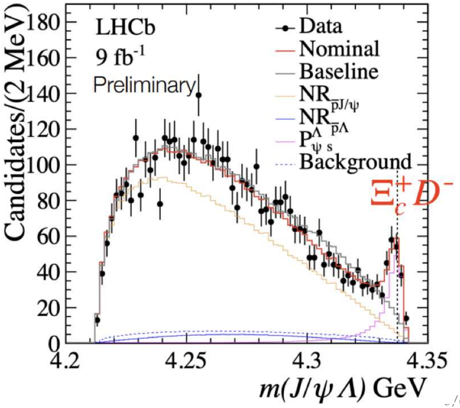

Objective

Analytic structure of the S-matrix and shape of poles

Energy Region	Analytic Structure of RS	Shape of Peak
Distant from threshold	Trivial ('flat') in Energy	Breit-Wigner O
Near threshold	Non-trivial in Energy	Breit-Wigner ✕

Objective

Clarify analytic stucture of 2, 3-channel S-matrix: draw a "map" of the S-matrix

Near-threshold spectrum decomposition & extraction of pole properties

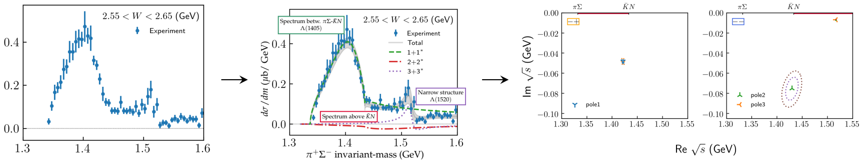

- Uniformization: mapping the non-trivial analytic structure of S-matrix
- Mittag-Leffler Expansion: pole expansion of meromorphic functions

Uniformization and Mittag-Leffler expansion: single-channel

Uniformization: "unfolding" the Riemann surface

- Analytic structure: Square-root type branch on the complex energy plane
- Uniformization with CM momenta k

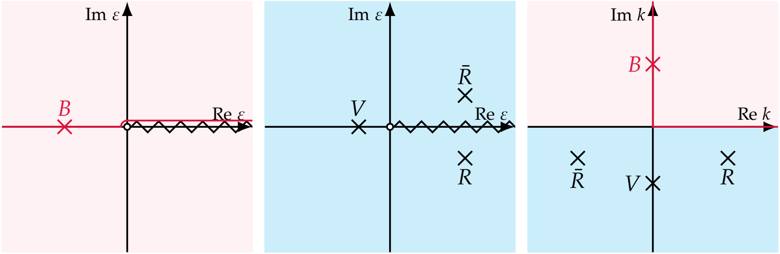

- Mittag-Leffler Expansion (ML Expansion)

  J. Humblet, L.Rosenfeld, Nucl. Physics 26 (1961)
  D. Ramírez Jiménez, N. Kelkar, Annals of Physics 396, 18 (2018)

$$\mathcal{A}(k) = \sum_n \left[\frac{r_n}{k - k_n} - \frac{r_n^*}{k + k_n^*} \right] + [\text{subtractions (entire function)}]$$

→ Extension to coupled-channel systems

S-matrix: 2-channel (2-body)

Energy plane

- Branch points at ϵ_1 and ϵ_2
- 4 sheets: $[tt]$, $[bt]$, $[tb]$, $[bb]$

  e.g. $[tb]_+$ means $\mathrm{Im}\, k_1 > 0$, $\mathrm{Im}\, k_2 > 0$, and $\mathrm{Im}\varepsilon > 0$

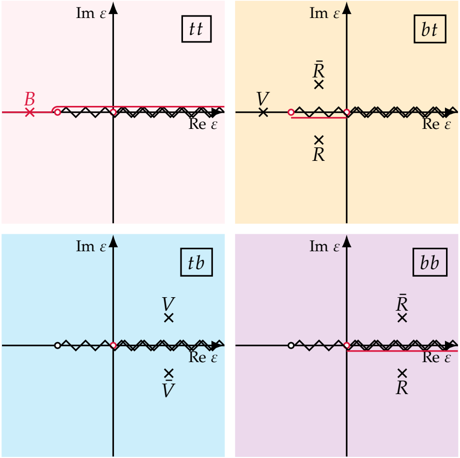

- Gluing condition at ϵ_1:

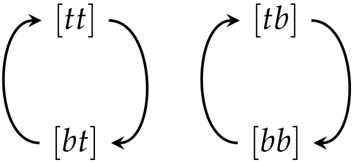

- Gluing condition at ϵ_2:

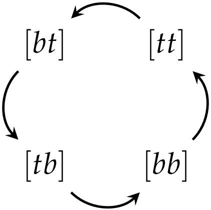

Riemann Sphere representation of the 2-channel S-matrix

- 2-channel $\mathcal{S}$-matrix $\simeq$ Sphere, $\mathbb{CP}^1$

z-plane M. Kato, Annals of Physics 31, 130 (1965)

$[tt]$, $[bt]$, $[tb]$, $[bb]$, e.g. $[tb]_+$ means $\mathrm{Im}\, q_1 > 0$, $\mathrm{Im}\, q_2 > 0$, and $\mathrm{Im}\,\varepsilon > 0$

$$z = \frac{1}{\Delta}(k_1 + k_2), \quad k_i = (\epsilon - \epsilon_i)^{1/2}, \quad \Delta = (\epsilon_2^2 - \epsilon_1^2)^{1/2}$$

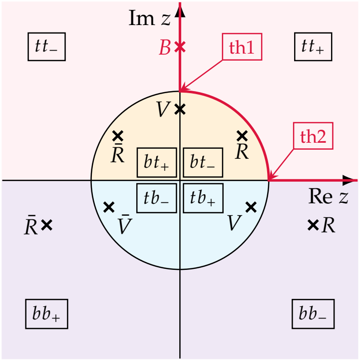

Mittag-Leffler Expansion on the Riemann Sphere

2-channel Mittag-Leffler Expansion

W. Yamada, O. Morimatsu, Phys. Rev. C 102, 055201 (2020)

$$\mathcal{A}(z) = \sum_i \left[\frac{r_n}{z - z_n} - \frac{r_n^*}{z + z_n^*} \right] + \text{(subtraction)}$$

Spectral decomposition invariant under: $Aut(\mathbb{CP}^1) \simeq PGL(2, \mathbb{C})$

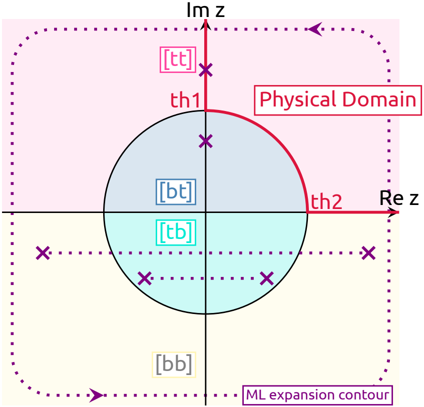

- Lone pole-pair contribution:

$$\mathcal{A}_n = \frac{r_n}{z - z_n} - \frac{r_n^*}{z + z_n^*}$$

$$\text{Im}\,\mathcal{A}_n(z) = \begin{cases} 0, & (\epsilon < \epsilon_1) \\ -\text{Im}\,\frac{2r_n}{(z_n - i)^2} \boxed{\frac{k_1}{\Delta}} + \mathcal{O}(k_1^2), & (\epsilon > \epsilon_1) \end{cases}$$

$$\text{Im}\,\mathcal{A}_n(z) =$$

$$\begin{cases} \text{Im}\,\frac{2r_n}{1 - z_n^2} - \text{Re}\,\frac{4r_n z_n}{(1 - z_n^2)^2} \boxed{\frac{\tilde{k}_2}{\Delta}} + \mathcal{O}(\tilde{q}_2^2), & (\varepsilon < \epsilon_2) \\ \text{Im}\,\frac{2r_n}{1 - z_n^2} - \text{Im}\,\frac{2r_n(1 + z_n^2)}{(1 - z_n^2)^2} \boxed{\frac{k_2}{\Delta}} + \mathcal{O}(q_2^2), & (\varepsilon > \epsilon_2) \end{cases}$$

2-channel Mittag-Leffler Expansion: Lineshapes

Lineshapes Pole contributions from pole-pair (pole and its "conjugate") with $|r_n| = 1$.

$$f(z; z_p, \phi_p) = -\frac{1}{\pi}\mathrm{Im}\left[\frac{\exp(i\phi_p)}{z - z_p} - \frac{\exp(-i\phi_p)}{z + z_p^*}\right]$$

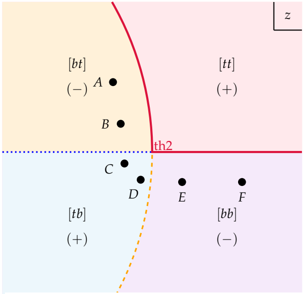

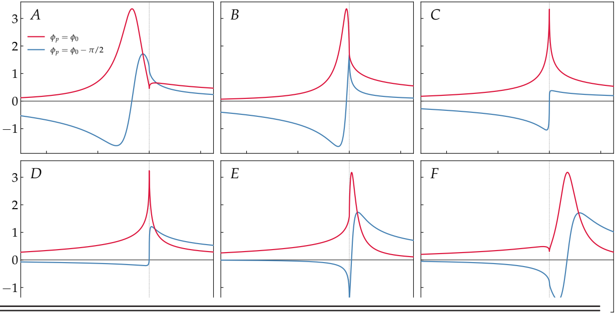

	A	B	C	D	E	F
z_p	$0.869 + 0.233i$	$0.895 + 0.094i$	$0.908 - 0.038i$	$0.962 - 0.092i$	$1.100 - 0.100i$	$1.300 - 0.100i$
e_p	$0.943 - 0.053i$	$1.000 - 0.022i$	$1.007 + 0.008i$	$0.992 + 0.007i$	$1.002 - 0.018i$	$1.065 - 0.043i$
e_0	0.933	0.989	1	1	1.01	1.065
γ_0	0.100	0.100	0.100	0.100	0.100	0.100
Sheet	[bt]	[bt]	[tb]	[tb]	[bb]	[bb]

- Peak position ≈ Closest Physical Point on z ($\neq$ Re E_R)
- Width of Structure $\propto$ Minimal Distance from Physical Domain on z ($\neq |\mathrm{Im}\ E_R|$)

Explicit ”Torus representation” of the 3-channel S-matrix

PRL 129, 192001 (2022)

$$z[\tau] = \frac{1}{4K(k)} \boxed{\int_0^{\gamma/z_{12}} \frac{d\xi}{\sqrt{1-\xi^2}\sqrt{1-k^2\xi^2}}}$$

Jacobi Elliptic integral

$$k = \frac{1}{\gamma^2},\ K(k) = \int_0^{\pi/2} \frac{d\theta}{\sqrt{1-k^2\sin^2\theta}},\ \tau = \frac{K(\sqrt{1-k^2})}{2K(k)}$$

$$\gamma = \left(\sqrt{\epsilon_3^2-\epsilon_1^2} + \sqrt{\epsilon_3^2-\epsilon_2^2}\right)/\sqrt{\epsilon_2^2-\epsilon_1^2}$$

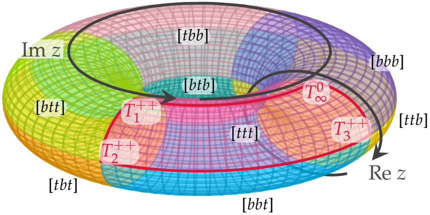

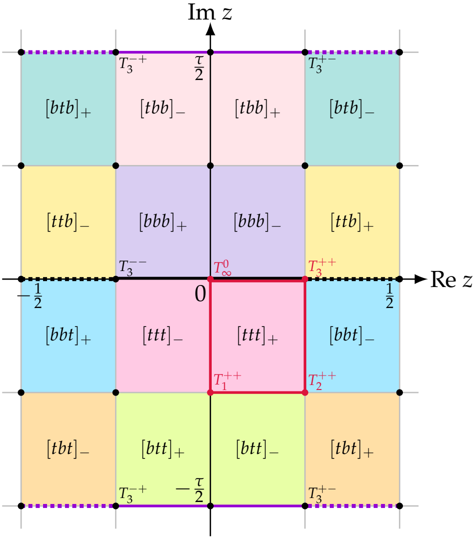

3-channel ML Expansion

Double Periodicity | Existance of "Mirror poles" → Naive pole expansion diverges

- Naive pole expansion + 1st, 2nd subtraction terms

$$\mathcal{A}(z) = \sum_{z_i \in \Lambda^*} \left[\frac{r_i}{z - z_i} + \sum_{m,n \neq 0} \frac{r_i}{z - z_i - \Omega_{mn}} \right] + [\text{subtractions}]$$

$$= C_0 + C_1 z + \sum_{z_i \in \Lambda^*} r_i \, \zeta(z - z_i)$$

Weierstrass Zeta function

$$\zeta(z) = \frac{1}{z} + \sum_{m,n \neq 0} \left[\frac{1}{z - \Omega_{mn}} + \frac{1}{\Omega_{mn}} + \frac{z}{\Omega_{mn}^2} \right]$$

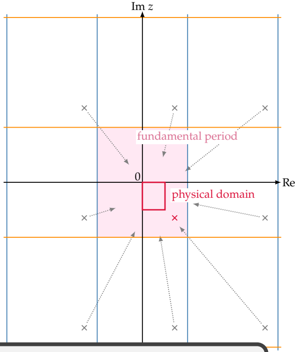

3-channel Mittag-Leffler Expansion under the Torus representation

$$\mathcal{A}(z) = \sum_{z_i \in \Lambda^*} r_i \left[\zeta(z - z_i) + \zeta(z_i) \right], \quad \sum_{z_i \in \Lambda^*} r_i = \frac{1}{2\pi i} \oint_{\partial \Lambda^*} dz \, A(z) = 0$$

Pole term

- Pole decomposition invariant under modular transformation $PGL(2, \mathbb{Z})$

Enhancement at the $D\bar{D}^*$ threshold

M. Ablikim et al., Phys. Rev. Lett. 110, 252001 (BESIII), M. Ablikim et al., Phys. Rev. Lett. 112, 022001 (BESIII), Z. Q. Liu et al., Phys. Rev. Lett. 110, 252002 (Belle)

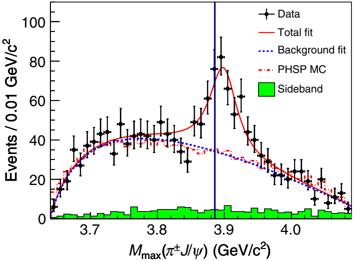

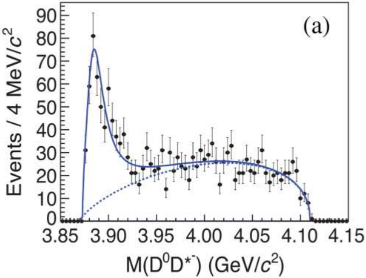

HALQCD: $\pi J/\psi$-$\rho\eta_c$-$D\bar{D}^*$, s-wave, (2+1)-flavor, m_π =410-700 MeV

Y. Ikeda, et.al., Phys. Rev. Lett. 117, 242001 (2016)

Case	[ttb]	[tbb]	[btb]
I	−146(112)(108) − i 38 (148)(32) −93(55)(21) − i 9(25)(7)	−177(116)(61) − i 175 (30)(22)	−369(129)(102) − i 207 (61)(20)
II	−102(84)(45) − i 14(11)(7) −59(67)(11) − i 3(12)(1)	−141(92)(64) − i 151 (149)(132)	−322(141)(111) − i 114 (96)(75)
III	−100(48)(29) −i 7(37)(17) −53(30)(5) −i 2(11)(3)	−127(52)(43) −i 199 (44)(28)	−356(108)(28) −i 277 (138)(95)

- Poles from the HALQCD result ($m_\pi = 411$ MeV) on the $\mathbb{CP}^1$ plane of channels $\pi J/\psi$ and $D\bar{D}^*$

$$e_p = (s_p - e_1^2)/(e_2^2 - e_1^2),$$
$$z_p = e_p^{1/2} + (e_p - 1)^{1/2}.$$
$e_1 = 3508$ MeV ($\pi J/\psi$), $e_2 = 3959$ MeV ($\bar{D}D^*$)

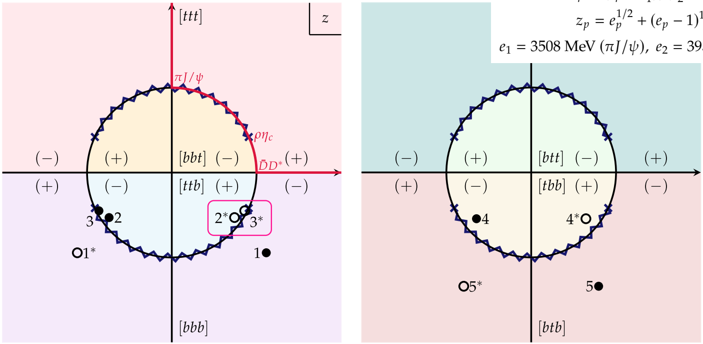

TABLE II. The uniformization variables, z_p, and the scaled energy, e_p, for S-matrix poles, 1–5 ($\mathrm{Im}\, e_p < 0$), given in Ref. [20], and for their conjugate poles, 1*–5* ($\mathrm{Im}\, e_p > 0$), not given in Ref. [20]. Also shown is the sheet on which each pole is positioned.

	$1, 1^*$	$2, 2^*$	$3, 3^*$	$4, 4^*$	$5, 5^*$
z_p	$\pm 1.11 - 0.95i$	$\mp 0.74 - 0.53i$	$\mp 0.86 - 0.45i$	$\mp 0.65 - 0.54i$	$\pm 0.79 - 1.34i$
e_p	$0.60 \mp 0.41i$	$0.66 \mp 0.09i$	$0.79 \mp 0.02i$	$0.60 \mp 0.17i$	$0.16 \mp 0.44i$
Sheet	$[bbb]$	$[ttb]$	$[ttb]$	$[tbb]$	$[btb]$

Z_c (3900)

- Separable potential model: $\pi J/\psi$-$\bar{D}D^*$ (HALQCD inspired)
  W. A. Yamada, O. Morimatsu, T. Sato, K. Yazaki Phys. Rev. D 105, 014034 (2022)

$$V_{ij}(p', p) = g(p')v_{ij}g(p),$$
$$g(p) = \frac{\beta^2}{\beta^2 + p^2},\ v_{11} = v_{22} = 0,\ v_{12} = v$$

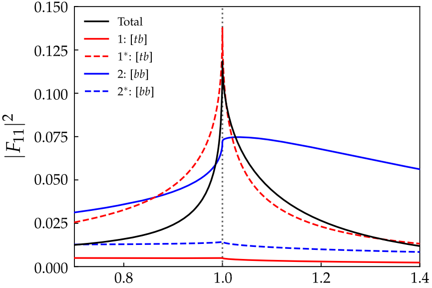

- Re-analysis of the HALQCD $\pi J/\psi$-$\rho\eta_c$-$D\bar{D}^*$ scattering amplitude (ongoing W. Yamada) on the torus: Magnitude of the residue of $[ttb]_+$ poles are a order or two larger than the other poles

Enhanced "threshold cusp" structure at $D\bar{D}^*$ threshold from poles on $[ttb]_+$

Time Evolution of Unstable states: Motivation

- Enhanced "cusp" at threshold coming from a pole on the unphysical sheet with a positive imaginary part in energy

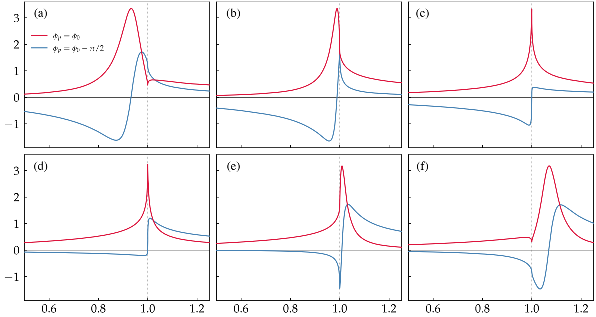

	A	B	C	D	E	F
z_p	$0.869 + 0.233i$	$0.895 + 0.094i$	$0.908 - 0.038i$	$0.962 - 0.092i$	$1.100 - 0.100i$	$1.300 - 0.100i$
e_p	$0.943 - 0.053i$	$1.000 - 0.022i$	$1.007 + 0.008i$	$0.992 + 0.007i$	$1.002 - 0.018i$	$1.065 - 0.043i$
e_0	0.933	0.989	1	1	1.01	1.065
γ_0	0.100	0.100	0.100	0.100	0.100	0.100
Sheet	$[bt]$	$[bt]$	$[tb]$	$[tb]$	$[bb]$	$[bb]$

- Study the time-dependence of a prepared state in systems where there are enhanced "cusp" poles

Survival amplitude: General behavior

Survival amplitude

$$\mathcal{A}(t) = \langle \psi(0) | \psi(t) \rangle$$
$$= \sum_B | \langle \psi(0) | B \rangle |^2 e^{-iE_B t} - \frac{1}{2\pi i} \int_0^\infty dE\, e^{-iEt} \mathrm{disc}\, \mathcal{G}(E)$$

- Small t: Non-exponential decay due to time-reversal invariance
- Intermidiate t: Exponential decay
- Large t ($\Gamma t \gg 1$): Only contribution from the end point (threshold)

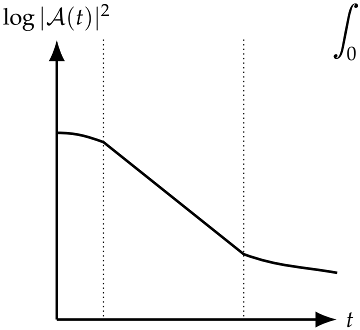

$$\int_0^{\pi/t} d\varepsilon\, \varepsilon^{l+1/2} e^{-it\varepsilon} \propto t^{-l-3/2}$$

- Short time: Quadratic decay ($t \sim 1/|E_R|$)
  Quantum Zeno Effect
- Intermidiate time: Exponential decay
- Large time: Inverse power decay
  L. A. Khalfin, Sov. Phys. JETP 6, 1053 (1958)

G. Ordonez and N. Hatano J. Phys. A 50, 40, 405304 (2017)

- 1D tight-binding model consisting of a quantum dot connected to two semi-infinite leads: *electron hopping from site to site*

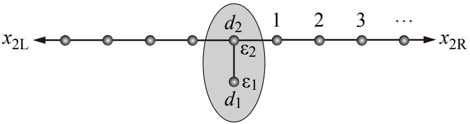

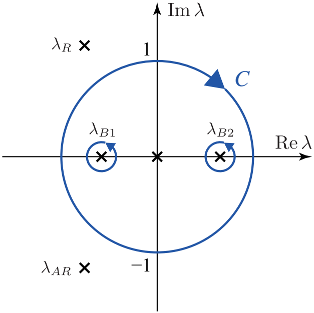

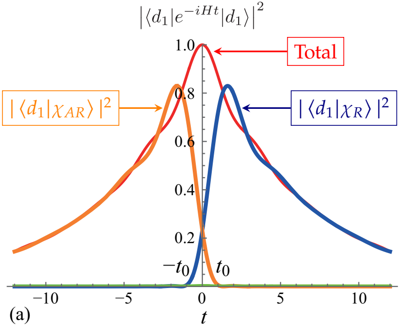

- Time-reversal symmetry

$$|\langle d_1|\chi_R(t)\rangle + \langle d_1|\chi_{AR}(t)\rangle|^2$$
$$= |\langle d_1|\chi_R(-t)\rangle + \langle d_1|\chi_{AR}(-t)\rangle|^2$$

- Exponential decay in intermidiate $t > 0$ ($t < 0$) region dominated by resonance (anti-resonance) contribution

"Survival Amplitude" in coupled-channels

Extension of Hatano-san's pole expansion to coupled-channel systems

Pole Expansion of "Survival Amplitude" (2-channel)

PRD 108, L071502(2023) W. Yamada, O. Morimatsu, T. Sato, K. Yazaki

Unstable state $|d_1\rangle$

$$\mathcal{A}(t) = \langle d_1|e^{-iHt}|d_1\rangle = \sum_B |\langle d_1|\phi_B\rangle|e^{-iE_Bt} + \boxed{\sum_n r_n \mathcal{A}_n(t;z_n)}$$

$$\mathcal{A}_n(t;z_n) = \frac{i}{4\pi}\left[\left(1-\frac{1}{z_n^2}\right)I(t;\varepsilon_n) + \left(1+\frac{1}{z_n^2}\right)e^{-it}I(t;\varepsilon_n-1) + \frac{2i}{z_n}J(t;\varepsilon_n)\right]$$

$$I(t;\varepsilon_n) = \sqrt{\frac{\pi}{it}} - i\pi\sqrt{\varepsilon_n}e^{-it\varepsilon_n}\mathrm{erfc}(i\sqrt{it\varepsilon_n}), \quad J(t;\varepsilon_n) = \int_0^1 d\varepsilon\,\frac{\sqrt{\varepsilon}\sqrt{1-\varepsilon}}{\varepsilon-\varepsilon_n}e^{-it\varepsilon}$$

- $I(t;\varepsilon_n)$ matches the analytic expression for the single-channel case
  Contributions from each channel (first term, second term)
- Interference term: $J(t;\varepsilon_n)$ involving both channels

“Survival Amplitude” in coupled-channels

Intermidiate t, pole near upper threshold i.e., $|\varepsilon_n - 1| \ll 1$

$$|\mathcal{A}_n(t > 0; z_n)|^2 \approx \frac{|r_n^k|^2}{\pi^2} |I(t; \varepsilon_n - 1)|^2$$

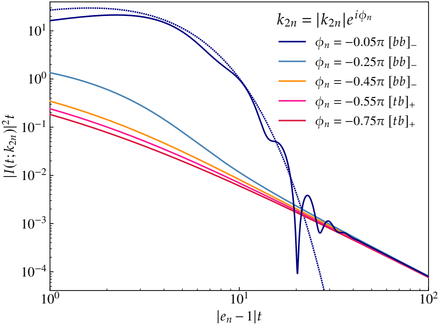

- Arg z dependence of $I(t, z)$ important
- Non-exponential decay when poles on $[tb]_+$ are dominant

Model: 2-channel Survival amplitude

Toy model Excited state coupled to two-channels

$$\hat{\mathcal{H}}_0 = \int \frac{d\vec{q}_1}{(2\pi)^3} q_1^2 \, |\vec{q}_1\rangle \langle \vec{q}_1| + \int \frac{d\vec{q}_2}{(2\pi)^3} (q_2^2 + \Delta^2) \, |\vec{q}_2\rangle \langle \vec{q}_2| + E_d \, |d\rangle \langle d| \, ,$$

$$\hat{\mathcal{V}} = g_1 \int \frac{d\vec{q}_1}{(2\pi)^3} v(q_1) \Big[|\vec{q}_1\rangle \langle d| + |d\rangle \langle \vec{q}_1| \Big] + g_2 \int \frac{d\vec{q}_2}{(2\pi)^3} v(q_2) \Big[|\vec{q}_2\rangle \langle d| + |d\rangle \langle \vec{q}_2| \Big],$$

$$v(k) = \frac{\mu^2}{k^2 + \mu^2}$$

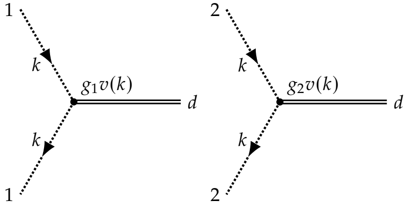

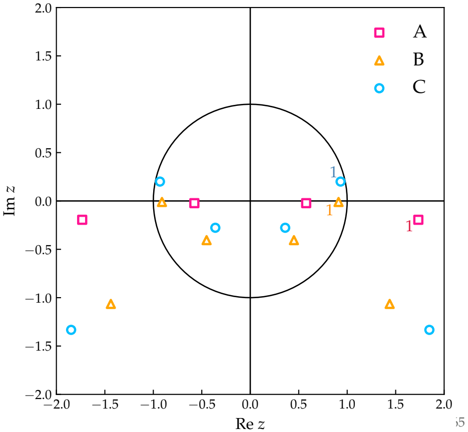

Change model parameters

- coupling constants: g_1, g_2
- Form factor cutoff: μ

$\longrightarrow$ case-A, case-B and case-C

“Survival Amplitude” of Unstable States

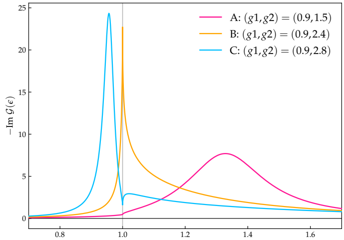

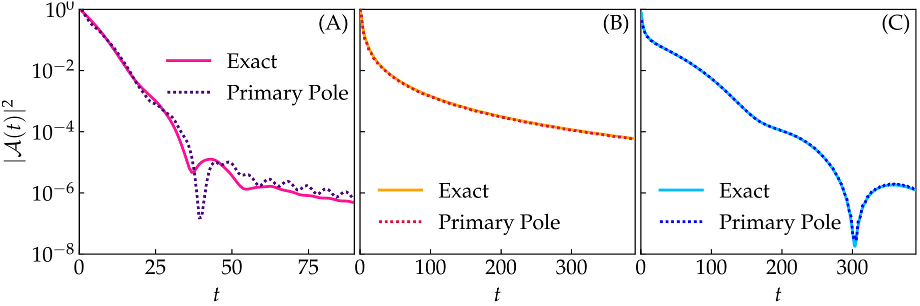

- Primary pole on $[bt]_{-}$, $[bb]_{-}$: Exponential decay → Inverse-power (t^{-3}) decay
- Primary pole on $[tb]_{+}$: Non-Exponential decay in all time regions

Pole expansion: correlation functions in Eucledian time

Eucledian correlation function of operators $\mathcal{O}^i$ and $\mathcal{O}^j$

$$C_E^{ij}(\tau) = \langle 0|\mathcal{O}^i(\tau)\mathcal{O}^j(0)|0\rangle = \int_{-\infty}^{\infty} \frac{dq_4}{2\pi} e^{iq_4\tau} D_E^{ij}(q_4)$$

$$D_E^{ij}(q_4) = -D^{ij}(q_0), \quad q_4 = iq_0$$

GS saturation

$$\langle 0|\mathcal{O}(\tau)\mathcal{O}(0)|0\rangle \to \mathcal{N} e^{-E_{\rm gs}\tau} \qquad (\text{large } \tau)$$

Objective Using the Mittag-Leffler expansion:

- Study the intermidiate time behavior
- Extract resonance information e.g., complex energy, residues, coupling constants from Eucledian correlation functions calculated in Lattice simulations

- Demonstration by Model: ρ meson model

Demonstration by ρ

Setup

Consider the correlations of operators $\mathcal{O}^\rho, \mathcal{O}^{\pi\pi}$

$$C_E(\tau) = \begin{bmatrix} \langle \mathcal{O}^\rho \mathcal{O}^\rho \rangle & \langle \mathcal{O}^\rho \mathcal{O}^{\pi\pi} \rangle \\ \langle \mathcal{O}^{\pi\pi} \mathcal{O}^\rho \rangle & \langle \mathcal{O}^{\pi\pi} \mathcal{O}^{\pi\pi} \rangle \end{bmatrix}$$

where

$$\mathcal{O}^\rho = \rho_3(\vec{q}, \tau) \qquad\qquad (\vec{q} = \vec{p}_1 + \vec{p}_2)$$

$$\mathcal{O}^{\pi\pi} = \frac{1}{\sqrt{2}}(\pi^-(\vec{p}_1, \tau)\pi^+(\vec{p}_2, \tau) - \pi^+(\vec{p}_1, \tau)\pi^-(\vec{p}_2, \tau))$$

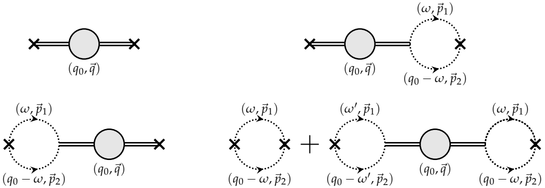

- Fixed 3-momenta, integration of energy in the pion loops
- poles in $D^{\rho\rho}$ and the $\pi\pi$ loop

Demonstration by ρ

If $D^{\rho\rho}$ is well expressed by one (pair) of poles

$$C_E^{\rho\rho} \approx r_\rho^{\rho\rho} C(\tau, k_\rho) - r_\rho^{\rho\rho *} C(\tau, -k_\rho^*)$$

$$C_E^{\rho\pi\pi} \approx r_\rho^{\rho\pi\pi} C(\tau, k_\rho) - r_\rho^{\rho\pi\pi *} C(\tau, -k_\rho^*) + r_{\pi\pi}^{\rho\pi\pi} C(\tau, k_{\pi\pi}) - r_{\pi\pi}^{\rho\pi\pi *} C(\tau, -k_{\pi\pi})$$

$$C_E^{\pi\pi\pi\pi} \approx r_\rho^{\pi\pi\pi\pi} C(\tau, k_\rho) - r_\rho^{\pi\pi\pi\pi *} C(\tau, -k_\rho^*) + r_{\pi\pi}^{\pi\pi\pi\pi} C(\tau, k_{\pi\pi}) - r_{\pi\pi}^{\pi\pi\pi\pi *} C(\tau, -k_{\pi\pi}) + s_{\pi\pi}^{\pi\pi\pi\pi} C'(\tau, k_{\pi\pi}) + s_{\pi\pi}^{\pi\pi\pi\pi *} C'(\tau, -k_{\pi\pi})$$

where

$$C(\tau, k_n) = \int_{-\infty}^{\infty} \frac{dq_4}{2\pi} \frac{e^{iq_4\tau}}{k(q_4) - k_n} \quad C'(\tau, k_n) = \int_{-\infty}^{\infty} \frac{dq_4}{2\pi} \frac{e^{iq_4\tau}}{(k(q_4) - k_n)^2}$$

- By fitting the correlation functions C_E, one can obtain the pole position k_ρ and residues $\{r_\rho\}$ (pole position $k_{\pi\pi}$ known)
- Residues $r_{\pi\pi}$ in CM frame $p_1 = p_2 = 0$ are related to scattering quatities (scattering volume of p-wave $\pi\pi$ scattering)
  It can be shown by studying the large τ behavior of $C_E^{\rho\pi\pi}$ (Miani, Testa, 1990)

Model setup Nucl. Phys. A560 411-436 (1993)

$$L_{\text{eff}} = g\epsilon^{abc}(k_1 - k_2)\rho^a_\mu(p)\pi^b(k_1)\pi^c(k_2)$$

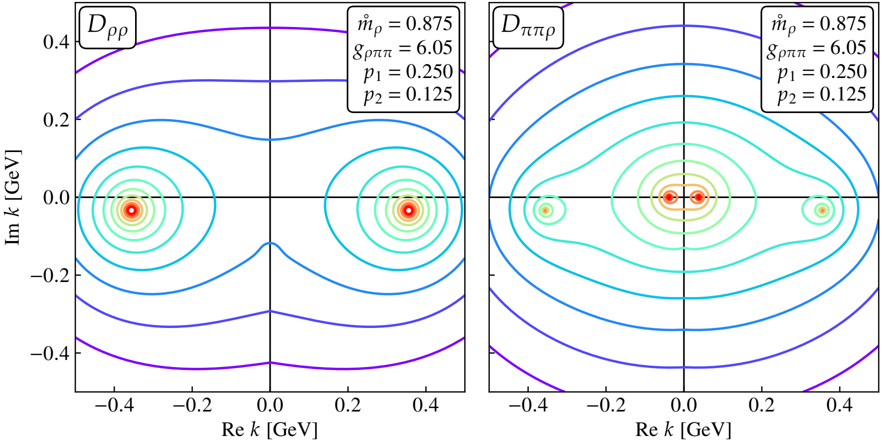

ρ meson Model

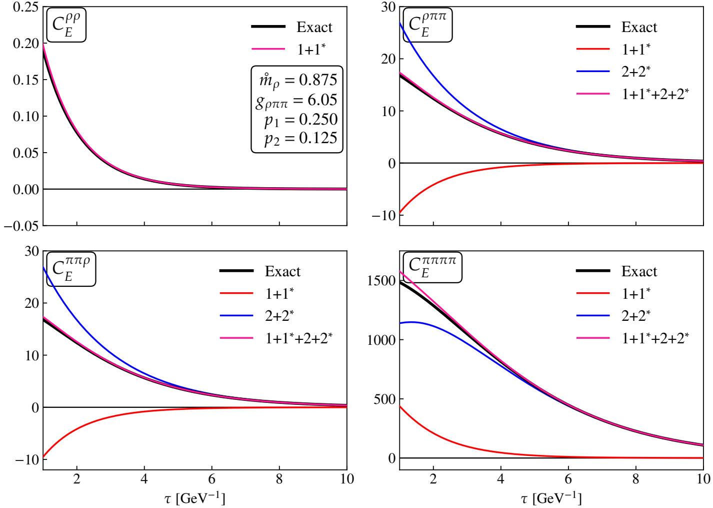

- Well expressed by the Mittag-Leffler expansion with the ρ pole and the $\pi\pi$ pole (and its conjugate poles)

Conclusion

Mittag-Leffler Expansion and Near-Threshold Spectrum

- Mittag-Leffler Expansion: accounts the non-trivial analytic structure of S-matrix, unique decomposition (Independent of the choice of the uniformization plane)
- Uniformization; 2-channel S-matrix: Sphere (3-channel S-matrix: Torus)
- Enhanced peak structure indicates the existance of a pole (poles)
  "Resonance": pole on $[bt]_-$, $[bb]_-$, "Threshold Cusp": pole on $[tb]_+$

Time Evolution survival amplitude of a 2-channeled system

- Decaying contributions for both resonance and "threshold cusp" poles
- For resonance poles, Exponential decay.
  For enhanced "threshold cusps" poles, there is no exponential decay for all time regions

MLE to temporal correlation functions

- Eucledian correlation functions are explicitly written as a pole expansion in terms of the pole positions (complex energy) and its residues under the uniformization variable
- Future projects: extension to coupled channels, finite volume effects, application to actual LQCD data

Backup

Uniformization

- Riemann surface = 1-demensional smooth manifold
- "Sheets" of Riemann surface ↔ Local charts defined on the manifold

Uniformization

- Construction of a global chart which covers the entire compact Riemann surface of interest (Some finite points may be omitted)

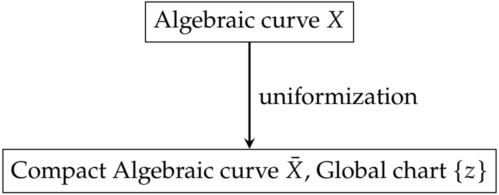

- Let us call the global chart as "uniformization variable"

Monodromy: gluing of local charts

Compact Riemann surface Riemann mapping theorem

Donaldson, S. K. (2011). *Riemann surfaces*. Oxford University Press. sec. 4.2.2

The (global) analytic structure is totally determined by

- Position of the branch points
- Elements of symmetric group S_n assigned to each branch point

Algebraic curve: $z - w^2 = 0$

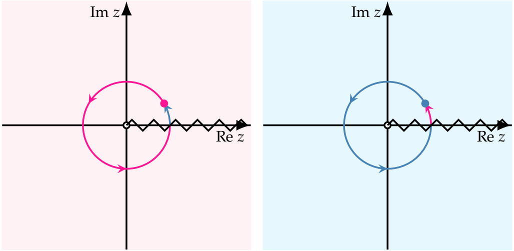

- Branch point: $z = 0$

$$\sigma(0) = \begin{pmatrix} 1 & 2 \\ 2 & 1 \end{pmatrix}$$

S-matrix: two-body, single-channel

Riemann Surface of the two-body single-channel S-matrix in the Energy plane

- Branch point at threshold energy $\epsilon_1 = m_1 + m_2$
- Monodromy the same as $z - w^2 = 0$

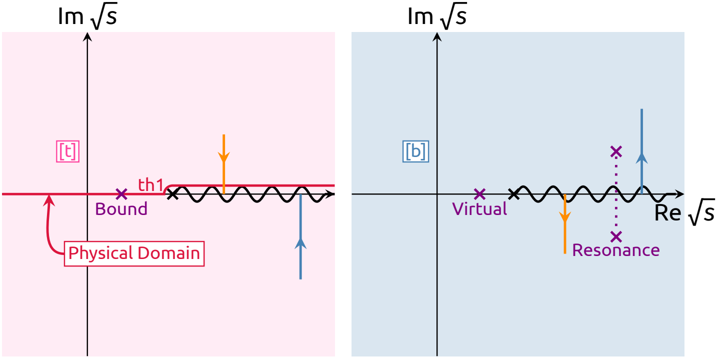

- momentum k is a uniformization variable of the two-body single-channel S-matrix

Mittag-Leffler expansion: two-body, single-channel

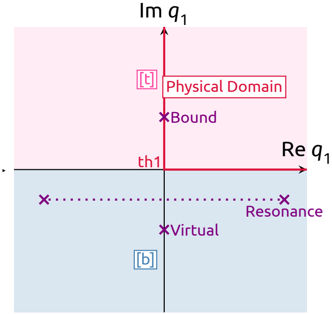

Mittag-Leffler Expansion (ML Expansion)

J. Humblet, L.Rosenfeld, Nucl. Physics 26 (1961)

D. Ramírez Jiménez, N. Kelkar, Annals of Physics 396, 18 (2018)

$$\mathcal{A}(k) = \sum_n \boxed{\left[\frac{r_n}{k - k_n} - \frac{r_n^*}{k + k_n^*} \right]} + \text{[subtractions (entire function)]}$$

Pole term

- Systematic extraction of the pole properties (positions, residues) based on general analytic properties of the S-matrix

Uniqueness of MLE Pole Decomposition on Sphere

2-channel uniformization plane: non-unique, infinite choices

Smooth bijective mapping $\mathbb{CP}^1 \to \mathbb{CP}^1$ induces new uniformization plane

Möbius transformation $\leftarrow$ only possible holomorphic mapping

$$Aut(\mathbb{CP}^1) \cong PGL(2, \mathbb{C})$$

$$z \mapsto w = \frac{\alpha z + \beta}{\gamma z + \delta}, \text{ where, } det \begin{bmatrix} \alpha & \beta \\ \gamma & \delta \end{bmatrix} \neq 0$$

which is a combination of,

1. translation: $z \mapsto z + a,\ a \in \mathbb{C}$ $\leftarrow$ trivial
2. homothety and rotation: $z \mapsto \lambda z,\ 0 \neq \lambda \in \mathbb{C}$ $\leftarrow$ trivial
3. inversion: $z \mapsto z^{-1}$ $\leftarrow$ can be easily shown

MLE Pole decomposition invariant under $\mathbb{CP}^1 \to \mathbb{CP}^1$ transformations

i. e. results from the Mittag-Leffler expansion does not depend on the choice of the uniformization plane

- One can also show that the MLE Pole decomposition is invariant under $\mathbb{CP}^1 \leftrightarrow \mathbb{C}/\mathbb{Z}$ and $\mathbb{C}/\mathbb{Z} \to \mathbb{C}/\mathbb{Z}$

3-channel S-matrix

2-sheeted z_{12}-plane (z-plane using channel mass ϵ_1, ϵ_2)

$$q_1 = \frac{\Delta_{12}}{2}\left[z_{12} + 1/z_{12}\right], \quad q_2 = \frac{\Delta_{12}}{2}\left[z_{12} - 1/z_{12}\right], \quad q_3 = \frac{\Delta_{12}}{2z_{12}}\underbrace{\sqrt{(1 - z_{12}^2\gamma^2)(1 - z_{12}^2/\gamma^2)}}_{\text{sq.root cut } z_{12} = \pm\gamma, \pm 1/\gamma}, \quad \left(\gamma = \frac{\sqrt{\epsilon_3^2 - \epsilon_1^2} + \sqrt{\epsilon_3^2 - \epsilon_2^2}}{\Delta_{12}}\right)$$

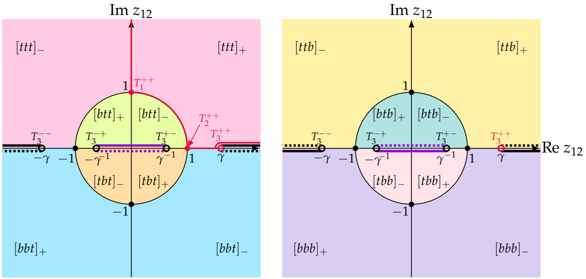

W.Y. O.M. T.S. arXiv:2203.17069 [hep-ph], Fig.1

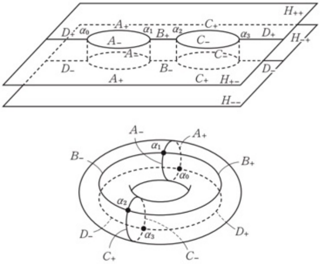

(楕円積分と楕円関数 おとぎの国の歩き方)

- 3-channel S-matrix has the structure of a Torus
  ↔ 2-channel S-matrix (Riemann Sphere)

H. Cohn, Conformal mapping on Riemann surfaces (Courier Corporation, 2014)
H. A. Weidenmüller Ann. Phys. (N.Y.) 28, 60 (1964)
R. G. Newton, Scattering Theory of Waves and Particles (Springer, 1982)

$\gamma p \to K^+ \pi \Sigma$

K. Moriya, et al. CLAS, PRC 87, 035206 (2013)

$K^- p \to K^- p, \bar{K}^0 n, \pi^\pm \Sigma^\mp$

Abrams et al. Phys. Rev. 139, B454 (1965), Bangerter et al. Phys. Rev. D 23, 1484 (1981), Ciborowski et al. J. Phys. G: Nucl. Phys. 8, 13 (1982), Csejthey-Barth et al. Phys.Lett. 16, 89 (1965), Humphrey et al. Phys. Rev. 127, 1305 (1962), Mast et al. Phys. Rev. D 14, 13 (1976), Sakitt et al. Phys. Rev. 139, B719 (1965)

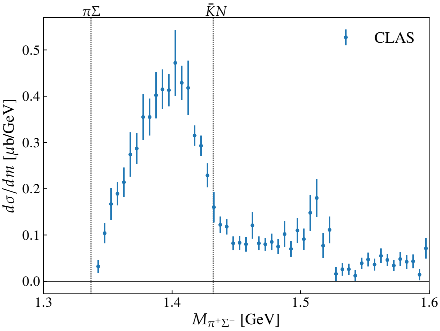

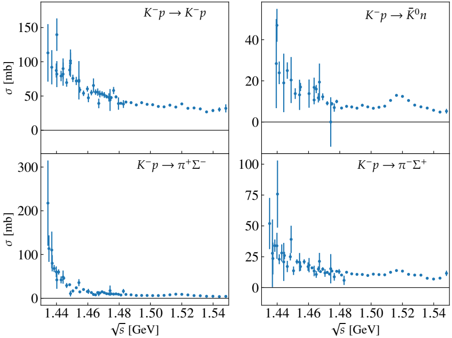

Wren Yamada, Osamu Morimatsu, PRC 103, 045201 (2021)

- 2-channel MLE on $\pi\Sigma$-$\bar{K}N$ sphere, common pole positions

$$\frac{d\sigma^{(\pi\Sigma)}}{dm} = \mathrm{Im}\sum\left[\frac{c_n^{(\pi\Sigma)}}{z-z_n} - \frac{c_n^{(\pi\Sigma)*}}{z+z_n^*}\right], \quad \sigma^{(if)} = \frac{k_f}{k_i}\mathrm{Im}\sum\left[\frac{c_n^{(if)}}{z-z_n} - \frac{c_n^{(if)*}}{z+z_n^*}\right]$$

Uniqueness of the MLE pole decomposition

we are able to truncate the Mittag-Leffler expansion without z-plane (uniformization plane) dependence

Scheme 1-pole MLE→2-pole MLE→3-pole MLE

check convergence of the pole position

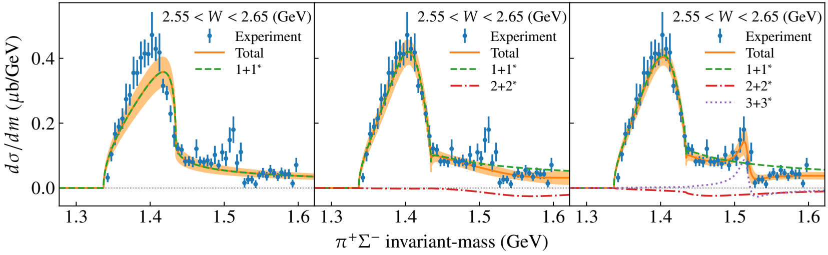

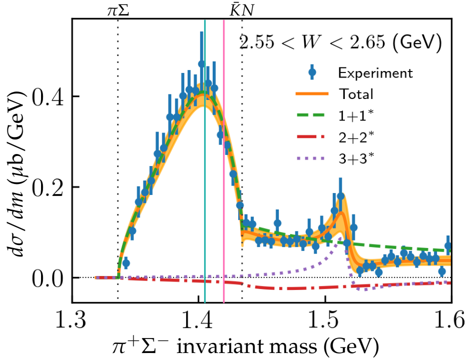

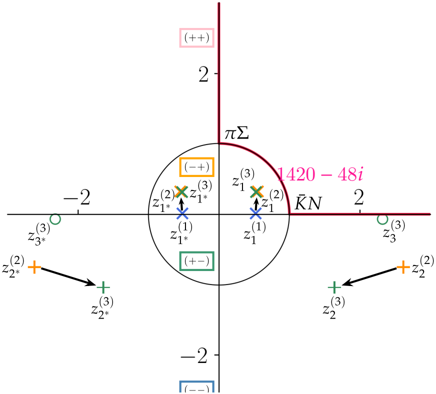

	Pole 1	Pole 2	Pole 3
$z_n^{(3)}$	$0.5243{+}0.3159i \pm 0.0062 \pm 0.0058i$	$1.6402{-}1.042i \pm 0.0684 \pm 0.0904i$	$2.3227 - 0.0687i \pm 0.0033 \pm 0.0031i$
$\sqrt{s_n^{(3)}}$	$1.4203{-}0.0475i \pm 0.0011 \pm 0.0015i$	$1.4283{-}0.074i \pm 0.01 \pm 0.0037i$	$1.5138 - 0.0068i \pm 0.0003 \pm 0.0003i$

Chiral unitary calculations

Y. Ikeda, T. Hyodo and W. Weise, Phys. Lett. B 706, 63 (2011)

Y. Ikeda, T. Hyodo and W. Weise, Nucl. Phys. A 881, 98 (2012)

Z.-H. Guo and J. Oller, Phys. Rev. C 87, 3, 035202 (2013)

M. Mai and U.-G. Meißner, Eur. Phys. J. A 51, 3, 30 (2015)

approach	pole 1 [MeV]	pole 2 [MeV]
Refs. [14, 15], NLO	$1424^{+7}_{-23} - i\ 26^{+3}_{-14}$	$1381^{+18}_{-6} - i\ 81^{+19}_{-8}$
Ref. [17], Fit II	$1421^{+3}_{-2} - i\ 19^{+8}_{-5}$	$1388^{+9}_{-9} - i\ 114^{+24}_{-25}$
Ref. [18], solution #2	$1434^{+2}_{-2} - i\ 10^{+2}_{-1}$	$1330^{+4}_{-5} - i\ 56^{+17}_{-11}$
Ref. [18], solution #4	$1429^{+8}_{-7} - i\ 12^{+2}_{-3}$	$1325^{+15}_{-15} - i\ 90^{+12}_{-18}$

$\pi^0\Sigma^0$ invariant distribution: GlueX

Future project

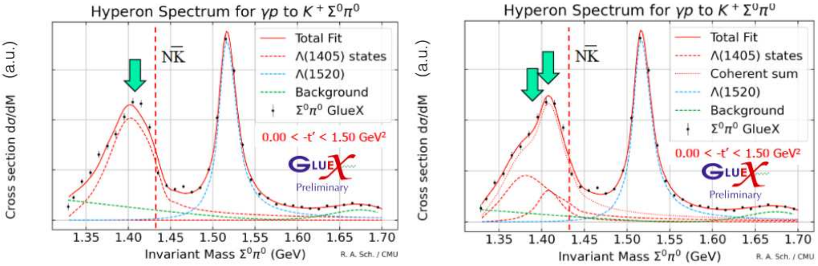

N. Wickramaarachchi, EPJ Web Conf. 271 (2022) 07005, HYP2022

- Possible to find Lower pole?

Model: $\Lambda\Lambda$-$N\Xi$-$\Sigma\Sigma$

Model: $\Lambda\Lambda$-$N\Xi$-$\Sigma\Sigma$ [$I = 0, J^P = 0^+$, Flavor singlet]

← simplified ver. of Y. Yamaguchi, T. Hyodo, Phys. Rev. C 94, 065207 (2016)

Bethe-Salpeter Eq., vertex from the group representation, only residual part of the loop function

$$\mathcal{L}_{int} = -\frac{1}{2}[BB]^\dagger \hat{C}[BB], \quad \hat{C} = \frac{C}{8}\begin{bmatrix} 1 & 2 & -\sqrt{3} \\ 2 & 4 & -2\sqrt{3} \\ -\sqrt{3} & -2\sqrt{3} & 3 \end{bmatrix}$$

$$i\hat{A} = -i\hat{C}\left[1 - \hat{G}\hat{C}\right]^{-1}, \quad G_i = -i\mu_i k_i/2\pi$$

BB: double-baryon fields, $\Lambda\Lambda$, $N\Xi$, $\Sigma\Sigma$

- For the s-wave amplitude, only one model parameter, C: ”coupling strength”
- 4 poles
- Validity check of the 3-channel Mittag-Leffler Expansion

Case (a): C=20 GeV^{-2}

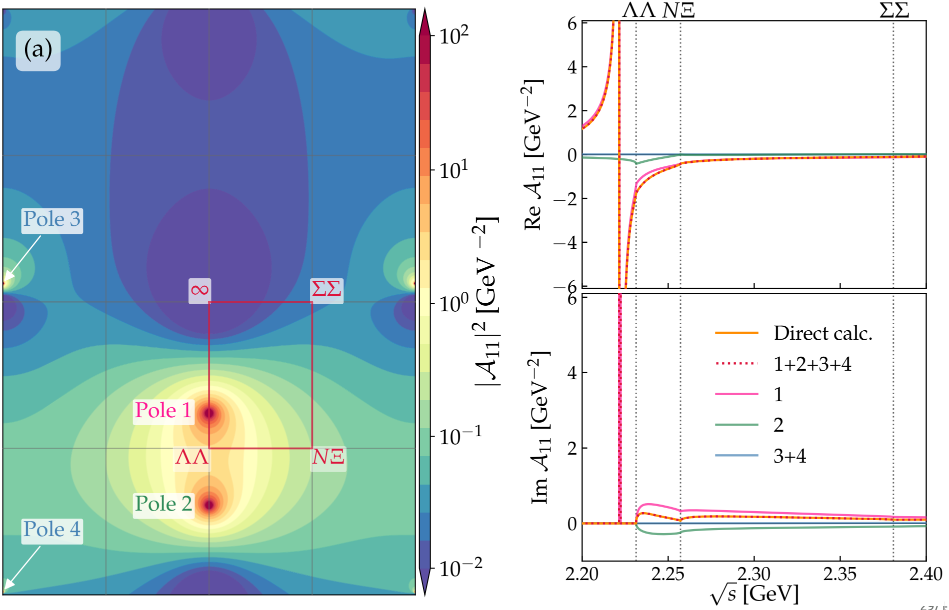

Case (b): C=22.65 GeV^{-2}

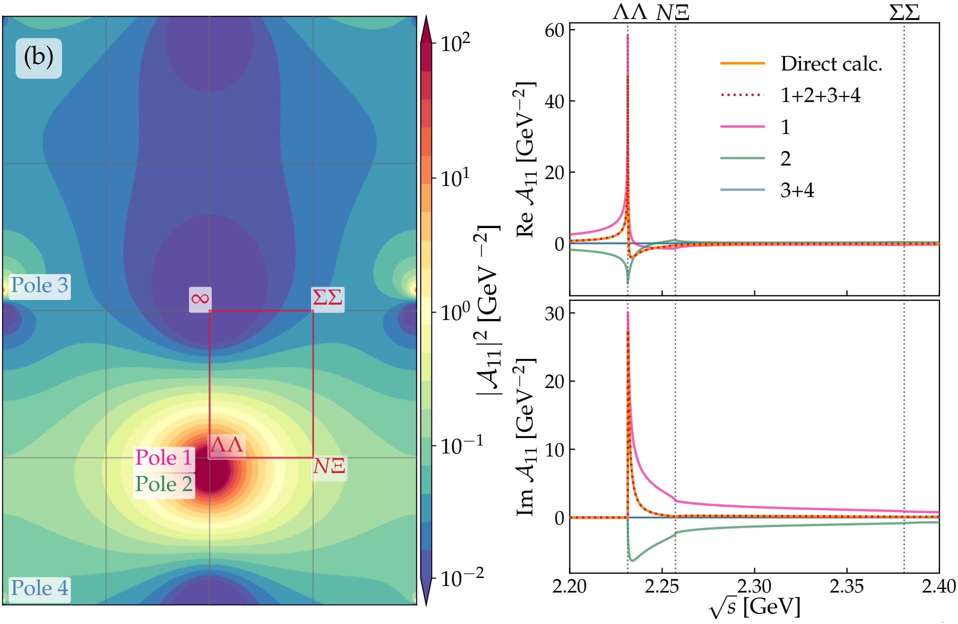

Case (c): C=30 GeV^{-2}

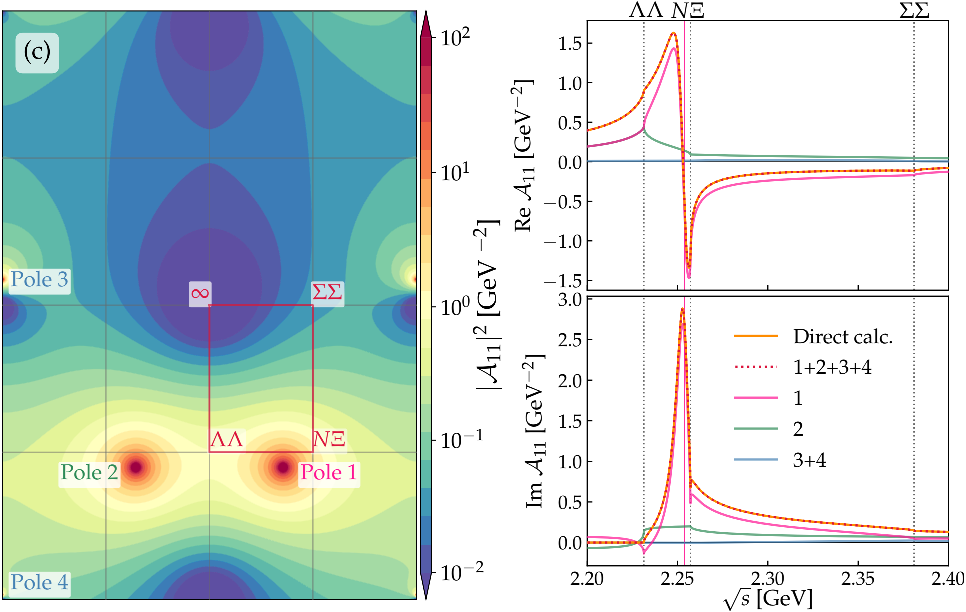

Case (d): C=40 GeV^{-2}

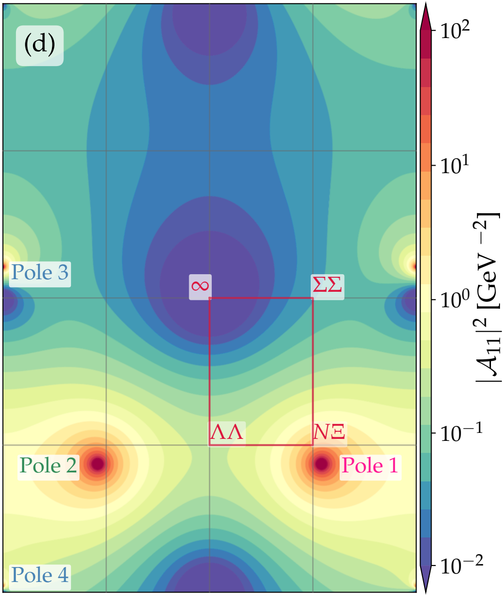

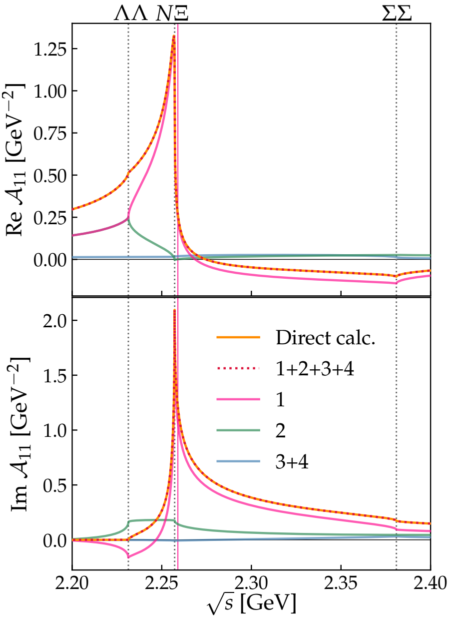

Model: $I=1$ $\pi\Lambda$-$\pi\Sigma$-$\bar{K}N$

Chiral-Unitary Model $\pi\Lambda$ (chn=1), $\pi\Sigma$ (chn=2), $\bar{K}N$ (chn=3)

- Interaction: Tomozawa-Weinberg (On-shell factorization)

$$V_{ij}(\sqrt{s}) = -\alpha \frac{C_{ij}}{4f^2}(2\sqrt{s} - M_i - M_j)\sqrt{\frac{E_i+M_i}{2M_i}}\sqrt{\frac{E_j+M_j}{2M_j}}, \quad C_{ij} = \begin{bmatrix} 0 & 0 & -\sqrt{3/2} \\ 0 & 2 & -1 \\ -\sqrt{3/2} & -1 & 1 \end{bmatrix}$$

$f = 1.123 f_\pi$, $\sqrt{s}$: c.m. Energy, E : Baryon Energy, M (m) : Baryon (Meson) Mass

- Amplitude T: Bethe-Salpeter Eq. Ladder Approx.
  Renormalization of Meson-Baryon Loop: Dimensional regularization (μ = 630 MeV)

$$T = V + VGT$$

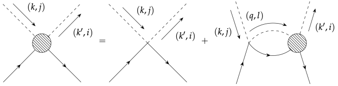

$$G = i\int \frac{d^4q}{(2\pi)^4}\frac{2M}{[(\sqrt{s}-q)^2 - M^2](q^2 - m^2)}$$

$$\rightarrow \frac{2M}{16\pi^2}\left[a(\mu) + \log\frac{M^2}{\mu^2} + \frac{m^2 - M^2 + s}{2s}\log\frac{m^2}{M^2} + \frac{\bar{q}}{\sqrt{s}}\log\frac{\phi_{++}\phi_{+-}}{\phi_{-+}\phi_{--}}\right]$$

$\phi_{\pm\pm} = \pm s \pm (M^2 - m^2) + 2\bar{q}\sqrt{s}$, $\bar{q}$: 3-momentum in c.m. frame

$a_{\pi\Lambda}$	$a_{\pi\Sigma}$	$a_{\bar{K}N}$
-1.83	-2.00	-1.84

$a_{\pi\Lambda}$, $a_{\pi\Sigma}$, $a_{\bar{K}N}$ from...

T. Hyodo, D. Jido Prog. Part. Nucl. Phys. 67, 55 (2012)

L. Roca, E. Oset PRC 88, 055206(2013)

Model: $I = 1$ $\pi\Lambda$-$\pi\Sigma$-$\bar{K}N$

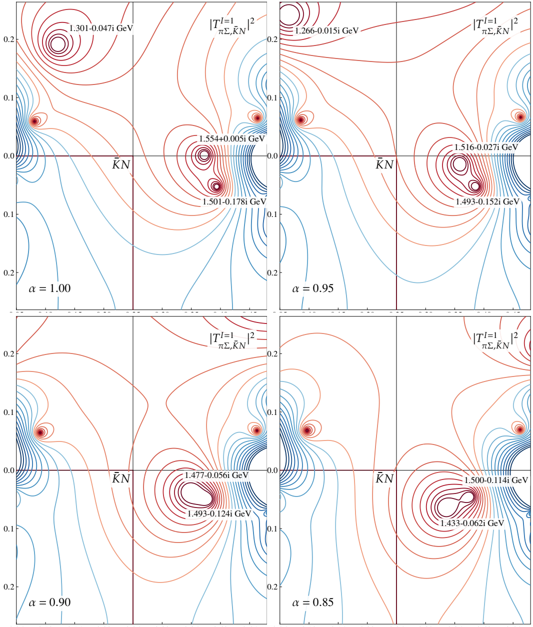

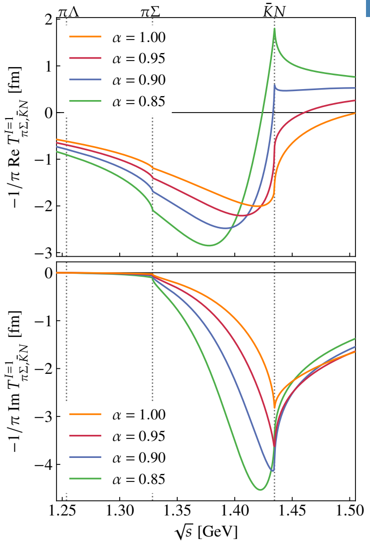

- Smooth transition from resonance pole to "cusp" pole when changing interaction strength

$\Xi(1620)$ MLE Fit (Preliminary)

- $\Xi_c^+ \to \Xi^- \pi^+ \pi^+$ Belle, M. Sumihama et. al., PRL 122, 072501 (2019)
- Torus of 3-channel system: $\pi^+\Xi^-$, $\bar{K}^0\Lambda$, $\bar{K}\Sigma$
- 3-pole Mittag-Leffler Expansion
- Mass resolution: $\sigma = 1.6$ MeV

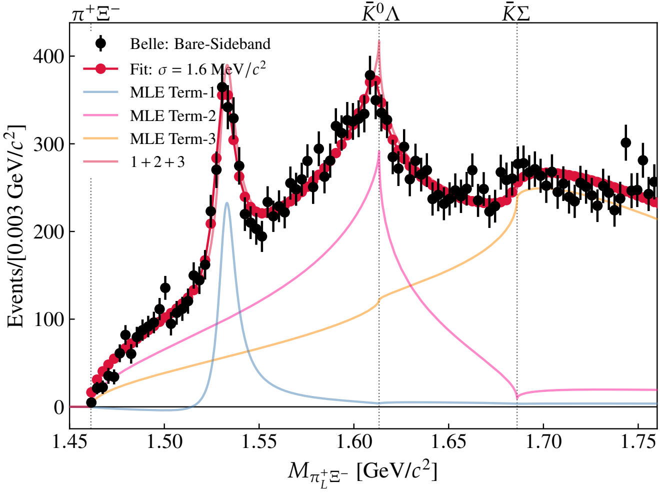

Ξ(1620) MLE Fit (Preliminary)

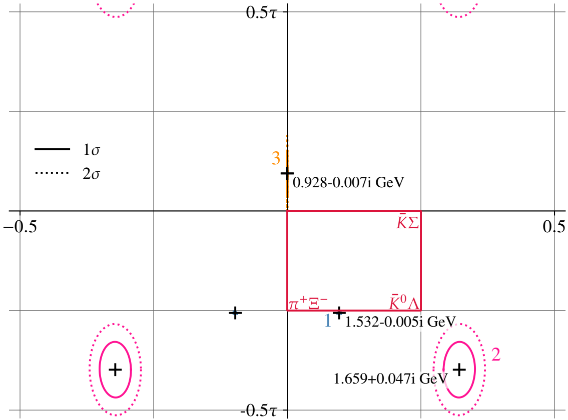

	Pole # 1	Pole # 2	Pole # 3
z	$0.097 - 0.220i \pm 0.003 \pm 0.002i$	$0.32 - 0.34i \pm 0.03 \pm 0.06i$	$0.00003 + 0.08i \pm 0.00003 \pm 0.05i$
ε_p [GeV]	$1.532 - 0.005i \pm 0.003 \pm 0.003i$	$1.66 + 0.05i \pm 0.05 \pm 0.03i$	$1 - 0.01i \pm 1 \pm 0.02i$
r_p^z [GeV^{-1}]	$-1.2 + 0.4i \pm 0.4 \pm 0.4i$	$-40 - 42i \pm 30 \pm 8i$	$-10000 + 41i \pm 9000 \pm 9i$
r_p^ε	$-1.2 + 0.4i \pm 0.4 \pm 0.4i$	$37 - 40i \pm 8 \pm 30i$	$-5000 + 200000i \pm 5000 \pm 200000i$

P_c MLE Fit (Preliminary)

- $\Lambda_b^0 \to pJ/\psi K^-$ LHCb, R. Aaij et al. Phys. Rev. Lett. 122, 222001 (2019)
- Torus of 3-channel system: pJ/ψ, $\Sigma_c^+\bar{D}^0$, $\Sigma_c^+\bar{D}^{*0}$
- 4-pole Mittag-Leffler Expansion
- Mass resolution: $\sigma = 2.0$ MeV

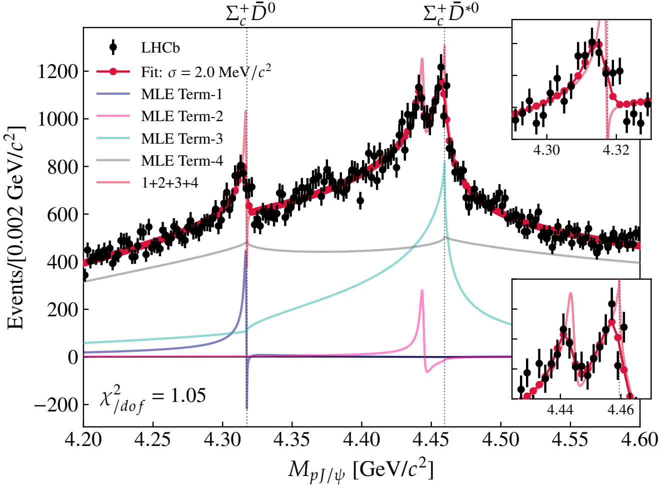

P_c MLE Fit (Preliminary)

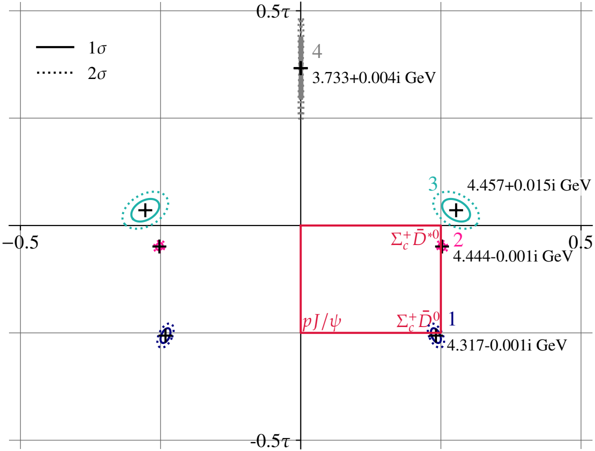

	Pole # 1	Pole # 2	Pole # 3	Pole # 4
z	$0.241 - 0.22i \pm 0.009 \pm 0.01i$	$0.252 - 0.042i \pm 0.006 \pm 0.007i$	$0.28 + 0.03i \pm 0.02 \pm 0.02i$	$0.000 + 0.32i \pm 0.004 \pm 0.06i$
ε_p [GeV]	$4.317 - 0.001i \pm 0.001 \pm 0.002i$	$4.444 - 0.001i \pm 0.005 \pm 0.004i$	$4.46 + 0.01i \pm 0.02 \pm 0.02i$	$3.7 + 0.00i \pm 0.6 \pm 0.04i$
r_p^z [GeV^{-1}]	$-1 - 3i \pm 4 \pm 3i$	$0.6 - 0.5i \pm 1.0 \pm 0.8i$	$40 - 1i \pm 20 \pm 30i$	$80 + 10i \pm 1000 \pm 20i$
r_p^ε	$0.1 - 0.5i \pm 0.4 \pm 0.4i$	$-0.3 - 0.4i \pm 0.5 \pm 0.7i$	$20 + 30i \pm 20 \pm 20i$	$-1200 + 8000i \pm 300 \pm 10000i$

Naive Interpretation: “$[tb]$” pole

<u>Naive description of the spacial distribution of “wave function”</u>

$$\psi(x) \sim e^{ik_p x}$$

- $[bb]$-pole

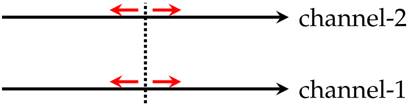

- $[bt]$-pole

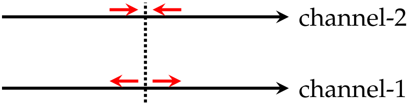

- $[tb]$-pole

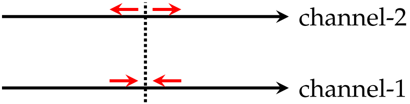

Time-Reversal Invariance

- Time-Reversal Operator T: anti-linear, commutes with the hamiltonian $[T, H] = 0$

$$T\,|\psi(t)\rangle = Te^{-iHt}\,|\psi(0)\rangle = e^{iHt}T\,|\psi(0)\rangle$$
$$|\psi(t)\rangle = Te^{iHt}T\,|\psi(0)\rangle \quad \because T^2 = 1$$

  A state that evolves forward in time (for t > 0) can be obtained by first time-reversing the initial state, next evolving it backwards in time, and finally reversing it again.

- If the initial state is even under time-reversal i.e. $T\,|\psi(0)\rangle = |\psi(0)\rangle$ Then,

$$\langle\psi(0)|\psi(t)\rangle = \langle\psi(0)|T|\psi(-t)\rangle = \langle\psi(0)|\psi(-t)\rangle^*$$
$$\mathcal{A}(t) = |\,\langle\psi(0)|\psi(t)\rangle\,|^2 = |\,\langle\psi(0)|\psi(-t)\rangle\,|^2$$

  <u>Survival amplitude $\mathcal{A}(t)$ invariant under time reversal</u>

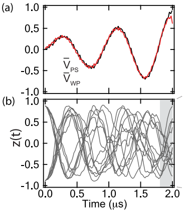

- N. Foroozani, M. Naghiloo, D. Tan, K. Mølmer, and K. W. Murch, Phys. Rev. Lett. 116, 110401 (2016): exponentially growing (decaying) Rabi oscillation signal when choosing final (initial) condition

Time dependence of unstable state

Consider normal resonance,

$$P_R(t) = |\Psi_R(t)|^2 = |\Phi_R|^2 e^{2t\mathrm{Im}\varepsilon_R}, \quad (\mathrm{Im}\varepsilon_R < 0)$$

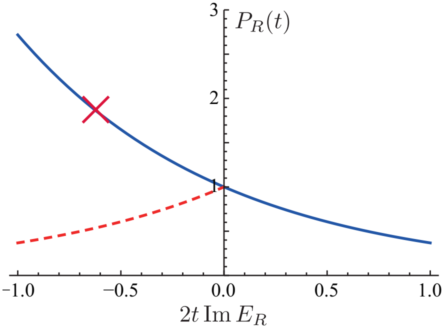

- Due to time-reversal invariance, $|\Psi(t)|^2$ cannot decay exponentially at arbitrary t
- The fact that the time evolution cannot be a genuine exponential decay, can also be shown from the Paley-Wiener theorem applied to the distribution $|\Psi|^2$
  Khalfin L A 1957 Zh. Eksp. Teor. Fiz. 33 1371

Gamow States in Rigged Hilbert Space

"Gamow states" defined in Rigged Hilbert Space (RHS)

- A. Bohm, J. Math. Phys. 22, 2813 (1981)
- O. Civitarese, and M. Gadella, Phys.Rept. 396 2, 41-113 (2004)

Rigged Hilbert Space (RHS)

$$\Phi_{\pm} \subset \mathcal{H}_{\pm} \subset \Phi_{\pm}^{\times}$$

$$\langle\tilde{\phi}_R| \in \Phi_{+},\ \ |\phi_R\rangle \in \Phi_{+}^{\times},\ \ \langle\tilde{\phi}_{AR}| \in \Phi_{-},\ \ |\phi_{AR}\rangle \in \Phi_{-}^{\times}$$

$$\langle\tilde{\phi}_R|\phi_R\rangle = 1,\ \ \langle\tilde{\phi}_{AR}|\phi_{AR}\rangle = 1$$

$$H\,|\phi_R\rangle = \varepsilon_R\,|\phi_R\rangle\,,\ H\,|\phi_{AR}\rangle = \varepsilon_{AR}\,|\phi_{AR}\rangle = \varepsilon_R^*\,|\phi_{AR}\rangle$$

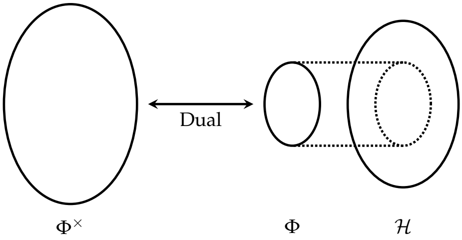

Gamow States in Rigged Hilbert Space

- "Completeness" Relation in Rigged Hilbert Space

$t < 0$

$$e^{-iHt}|\psi\rangle = \sum_B e^{-i\varepsilon_B t}|\phi_B\rangle\langle\phi_B|\psi\rangle + \boxed{\sum_R e^{-i\varepsilon_R^* t}|\phi_{AR}\rangle\langle\tilde{\phi}_{AR}|\psi\rangle}$$

Exponential growth from antiresonance

$$+\boxed{\int_0^{-\infty_{II}} d\varepsilon e^{-i\varepsilon t}|\varepsilon_{II}\rangle\langle\varepsilon_{II}|\psi\rangle}$$

$t > 0$

$$e^{-iHt}|\psi\rangle = \sum_B e^{-i\varepsilon_B t}|\phi_B\rangle\langle\phi_B|\psi\rangle + \boxed{\sum_R e^{-i\varepsilon_R t}|\phi_R\rangle\langle\tilde{\phi}_R|\psi\rangle}$$

Exponential decay from resonance

$$+\boxed{\int_0^{-\infty_{II}} d\varepsilon e^{-i\varepsilon t}|\varepsilon_{II}\rangle\langle\varepsilon_{II}|\psi\rangle}$$

- Existance of additional integral term (orange); deviation from a genuine exponential decay (growth) for $t > 0$ ($t < 0$). Only zero when $\langle\varepsilon_{II}|\psi\rangle$ $\forall\varepsilon \in (-\infty_{II}, 0) \rightarrow$ zero everywhere (Identity theorem) which is not physical

Survival Amplitude: Two-Channel Systems

Large t Method of Steepest descent

$$J(t;\varepsilon_n) = \int_0^1 d\varepsilon \frac{\sqrt{\varepsilon}\sqrt{1-\varepsilon}}{\varepsilon-\varepsilon_n} e^{-it\varepsilon}$$

$$\sim \frac{2e^{-it}}{1-\varepsilon_n}\int_0^\infty d\xi\, \xi^2 e^{it\xi^2} - \frac{2}{\varepsilon_n}\int_0^\infty d\xi\, \xi^2 e^{-it\xi^2} = \frac{\sqrt{\pi}}{2} t^{-3/2}\left[\frac{e^{-it}e^{-i\pi/4}}{-1+\varepsilon_n} + \frac{e^{i\pi/4}}{\varepsilon_n}\right]$$

$$\mathcal{A}_n(t) = \frac{i}{\sqrt{4\pi}} e^{i\pi/4} e^{-it/2} t^{-3/2}\left[e^{it/2}(z_n - i)^{-2} + e^{-it/2}(z_n-1)^{-2}\right] + \mathcal{O}(t^{-5/2}), \quad |t| \gg 1$$

$$|\mathcal{A}_n(t)|^2 \sim \frac{1}{4\pi}\frac{1}{|z_n - i|^2 |z_n - 1|^2}\left[\frac{|z_n-1|^2}{|z_n-i|^2} + \frac{|z_n-i|^2}{|z_n-1|^2} + \boxed{2\cos(t+\phi)}\right] t^{-3} + \mathcal{O}(t^{-4})$$

oscillating

- t^{-3} inverse-power law in the large-t region
- Oscillation during the entire inverse-power region
  $\leftrightarrow$ single-channel: Oscillation only during transition from exponential to inverse-power decay

Survival Amplitude: Two-Channel Systems

Intermidiate t

- Resonance, z_n on $[bt]_-$, $[bb]_-$, distant from thresholds;

$$\mathcal{G}_n = \frac{r_n}{z - z_n} \approx \frac{r_n^\varepsilon}{\varepsilon - \varepsilon_n}, \quad r_n^\varepsilon = \frac{1}{2} z_n (1 - z_n^{-2})$$

$$\boxed{|\mathcal{A}_n(t > 0; z_n)|^2 \approx |r_n^\varepsilon|^2 e^{2t \mathrm{Im} \varepsilon_n}}$$

- Enhanced "threshold cusp", z_n on $[tb]_+$, near upper threshold; $|\varepsilon_n - 1| \ll 1$

$$\mathcal{G}_n = \frac{r_n}{z - z_n} \approx \frac{r_n^k}{k - k_n}, \quad k = \frac{1}{2}(z - 1/z), \quad r_n^k = \frac{1}{2}(1 + z_n^{-2}),$$

$$\mathcal{A}_n(t > 0; z_n) \approx -\frac{r_n^k}{2i\pi} \left[\int_{-i\infty}^{0} dk \frac{2k}{k - k_n} e^{-it(1+k^2)} + \int_0^\infty dk \frac{2k}{k - k_n} e^{-it(1+k^2)} \right]$$

$$= \frac{i}{\pi} r_n^k e^{-it} I(t; \varepsilon_n - 1)$$

$$\boxed{|\mathcal{A}_n(t > 0; z_n)|^2 \approx \frac{|r_n^k|^2}{\pi^2} |I(t; \varepsilon_n - 1)|^2}$$

Argument dependence of Erfc → non-exponential decay for all time regions

G. Ordonez and N. Hatano: J. Phys. A 50, 40, 405304 (2017)

$P(t)$: Survival probability of the *'excited state'* $|d_1\rangle$ at a given time t. $P(0) = 1$.

$$\mathcal{A}(t) = \langle d_1|e^{-iHt}|d_1\rangle = \sum_n e^{-i\varepsilon_n t}\langle d_1|\phi_n\rangle\langle\phi_n|d_1\rangle + \sum_{a=L,R}\int_{-\pi}^{\pi}\frac{dk}{2\pi}e^{-i\varepsilon_k t}\langle d_1|\phi_{ka}\rangle\langle\phi_{ka}|d_1\rangle$$

$$= \int_C \frac{d\lambda}{2i\pi\lambda}\left[-\lambda + \frac{1}{\lambda}\right]e^{ib(\lambda+\lambda^{-1})t}\boxed{\frac{bg^2}{h(\lambda)f(\lambda)}}$$

$$= \sum_{n=1}^{2N}\langle d_1|\chi_n(t)\rangle$$

$$\lambda = e^{ik}, \quad \varepsilon = -b(\lambda+\lambda^{-1})$$

$$h(\lambda) = -b(\lambda+\lambda^{-1}) - \varepsilon_1,$$

$$f(\lambda) = h(\lambda)\left[-b(\lambda+\lambda^{-1}) - \varepsilon_2 + \lambda\sum_{a=L,R}\frac{t_{2a}^2}{b}\right] - g^2$$

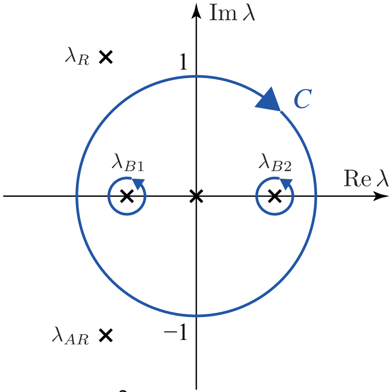

$$|\langle d_1|\chi_R(t)\rangle|^2 = |\langle d_1|\chi_{AR}(-t)\rangle|^2$$

$$|\langle d_1|\chi_R(t)\rangle + \langle d_1|\chi_{AR}(t)\rangle|^2 = |\langle d_1|\chi_R(-t)\rangle + \langle d_1|\chi_{AR}(-t)\rangle|^2$$

G. Ordonez and N. Hatano: J. Phys. A 50, 40, 405304 (2017)

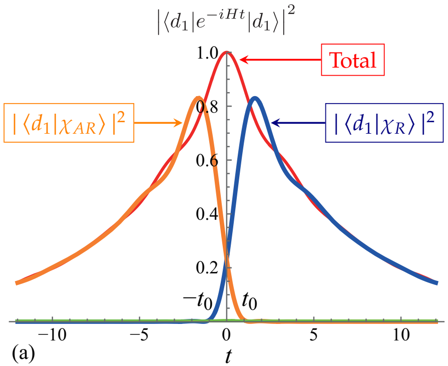

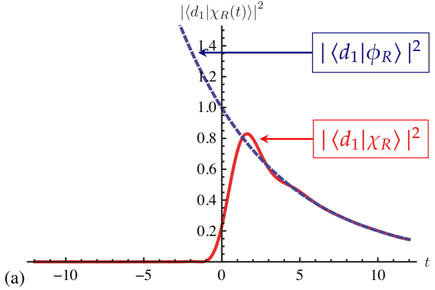

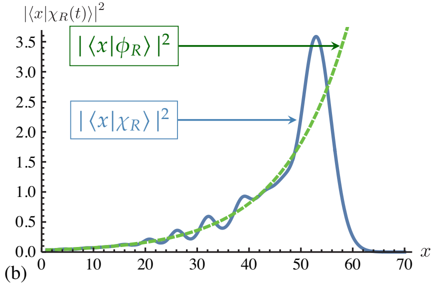

$$|\mathcal{A}(t)|^2 = |\mathcal{A}(-t)|^2$$

$$|\langle d_1|\chi_R(t)\rangle|^2 = |\langle d_1|\chi_{AR}(-t)\rangle|^2$$

- No exponential divergences for t, x

ρ meson Model

Model setup Nucl. Phys. A560 411-436 (1993)

$$L_{\text{eff}} = g\epsilon^{abc}(k_1 - k_2)\rho^a_\mu(p)\pi^b(k_1)\pi^c(k_2)$$

$$D(q_0, \vec{p}_1, \vec{p}_2) = \begin{bmatrix} D_\rho(q) & gD_\rho(q)\Lambda(q_0, \vec{p}_1, \vec{p}_2) \\ g\Lambda(q_0, \vec{p}_1, \vec{p}_2)D_\rho(q) & \Lambda(q_0, \vec{p}_1, \vec{p}_2) + g^2\Lambda(q_0, \vec{p}_1, \vec{p}_2)D_\rho(q)\Lambda(q_0, \vec{p}_1, \vec{p}_2) \end{bmatrix}$$

$$D_\rho(q) = [q^2 - \mathring{m}_\rho^2 - \Pi(q^2)]^{-1}$$

$$\Pi(q^2) = -\frac{g^2}{24\pi^2}q^2\left[\mathcal{G}(q^2, m_\pi^2) - \mathcal{G}(q^2, \Lambda^2) + \frac{4(\Lambda^2 - m_\pi^2)}{q^2} + \log\left(\frac{\Lambda}{m_\pi}\right)\right]$$

$$\mathcal{G}(q^2, m_\pi^2) = -\frac{1}{2}\left(1 - \frac{4m_\pi^2}{q^2}\right)^{3/2}\left[\log\frac{1 + (1 - 4m_\pi^2/q^2)^{1/2}}{1 - (1 - 4m_\pi^2/q^2)^{1/2}} - i\pi\right]$$

$$i\Lambda(q_0, \vec{p}_1, \vec{p}_2) = \frac{1}{4\omega_{p_1}\omega_{p_2}}\left[\frac{1}{q_0 - \omega_{p_1} - \omega_{p_2}} - \frac{1}{q_0 + \omega_{p_1} + \omega_{p_2}}\right]$$

- parameters: $g, \mathring{m}_\rho, m_\pi, \Lambda$
- poles in D_ρ and $\Lambda(q_0, \vec{p}_1, \vec{p}_2)$

ρ meson Model

D^{ij} on the real axis of $s^{1/2}$

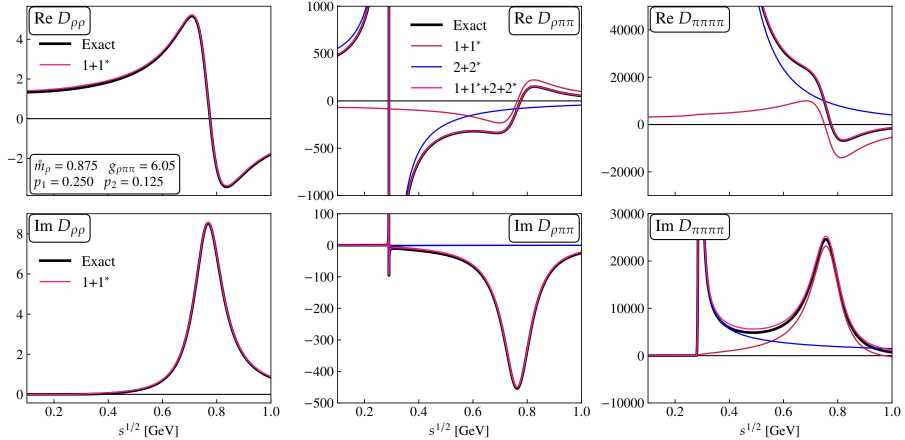

- Well expressed by the Mittag-Leffler expansion with the ρ pole and the $\pi\pi$ pole (and its conjugate poles)

ρ meson Model

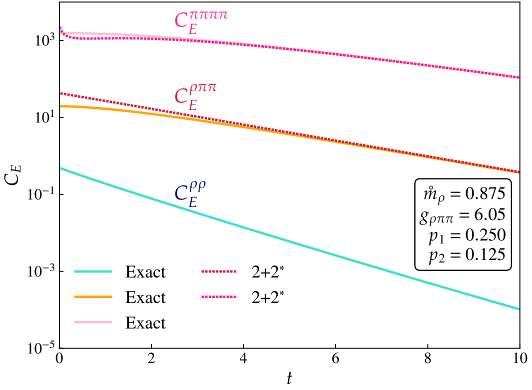

- $C_E^{\rho\pi\pi}, C_E^{\pi\pi\pi\pi}$ is domineted by the $\pi\pi$-pole contributions at large τ

Application Procedure

General procedure to extract resonance parameters from lattice data

1. Calculate (use lattice data of) $C_E^{\pi}(\tau, \vec{p})$ and $C_E^{\rho\rho}$, $C_E^{\rho\pi\pi}$, $C_E^{\pi\pi\rho}$, $C_E^{\pi\pi\pi\pi}$
2. Determine m_π and r_π from $C_E^{\pi}(\tau, \vec{p})$

$$C_E \approx r_\pi e^{-\varepsilon_\pi \tau} \; (\tau > 0), \quad \varepsilon_\pi = (m_\pi^2 + \vec{p}^2)^{1/2}$$

3. Construct uniformization variable k
4. $\pi\pi$-pole $k_{\pi\pi}$ is positioned at $q_0 = \omega_{p_1} + \omega_{p_2}$

   Fit the tail of $C_E^{\rho\pi\pi}$, $C_E^{\pi\pi\rho}$, $C_E^{\pi\pi\pi\pi}$ and determine $r_{\pi\pi}^{\rho\pi\pi}$, $r_{\pi\pi}^{\pi\pi\rho}$, $r_{\pi\pi}^{\pi\pi\pi\pi}$, $s_{\pi\pi}^{\pi\pi\pi\pi}$
5. Fit the remainder and determine the pole position k_ρ, and residues $r_\rho^{\rho\rho}$, $r_\rho^{\rho\pi\pi}$, $r_\rho^{\pi\pi\rho}$, $r_\rho^{\pi\pi\pi\pi}$

Application Procedure

General procedure to extract resonance parameters from lattice data

- Insensitivity of the imaginary part of complex energy

1. Determine cupling g:

$$r_\rho^{\rho\pi\pi} \approx g r_\rho^{\rho\rho} \Lambda(q_0, \vec{p}_1, \vec{p}_2)|_{k=k_\rho}, \quad r_\rho^{\pi\pi\pi\pi} \approx g^2 r_\rho^{\rho\rho} \Lambda(q_0, \vec{p}_1, \vec{p}_2)|_{k=k_\rho}$$

$$i\Lambda(q_0, \vec{p}_1, \vec{p}_2) = \int_{-\infty}^{\infty} \frac{d\omega}{2\pi} iD^\pi(\omega) iD^\pi(q_0 - \omega)$$

2. Determine Γ:

$$\Gamma \approx \frac{g^2}{6\pi} \frac{(m_\rho^2 - m_\pi^2)^{3/2}}{m_\rho^2}$$

  - future work: improvement of this relation

Extension to coupled-channels (Two channels)

- Uniformization variable z

$$z = \frac{(-q_4^2 - \vec{q}^2 - \varepsilon_1^2)^{1/2} + (-q_4^2 - \vec{q}^2 - \varepsilon_2^2)^{1/2}}{(\varepsilon_2^2 - \varepsilon_1^2)^{1/2}}$$

ε_1, ε_2: threshold energies

- Eucledian correlation function is written as a pole expansion using z

$$C_E^{ij}(\tau) = \sum_n r_n^{ij} C(\tau, z_n), \quad C(\tau, z_n) = -\int_{-\infty}^{\infty} \frac{dq_4}{2\pi} \frac{e^{iq_4\tau}}{z - z_n}$$

- Using this pole expansion, one should be able to obtain resonance parameters in the same way as the single-channel case
- Check with EFT Model of $\pi\eta$-$\bar{K}K$ ($I = 1$) Ongiong work

HAL potential: $\pi J/\psi$-$\rho\eta_c$-$D\bar{D}^*$ s-wave, $m_\pi = 411$ MeV

$$\mathcal{V}^{\alpha\beta}(r) \simeq \sum_{n=1}^{3} a_n e^{-b_n^2 r}$$

Pole position $T^{\pi J/\psi \pi J/\psi}$ on the torus